Scripta Materialia 155 (2018) 89–93

Contents lists available at ScienceDirect

Scripta Materialia

journal homepage: www.elsevier.com/locate/scriptamat

Regular Article

Twin-like fault in Mg–9.8 wt%Sn alloy

Chaoqiang Liu [a,b], Houwen Chen [a,c,*], Nick Wilson [d], Jian-Feng Nie [a,b,c,**]

[a] International Joint Laboratory for Light Alloys (Ministry of Education), College of Materials Science and Engineering, Chongqing University, Chongqing 400044, PR China
[b] Department of Materials Science and Engineering, Monash University, Victoria 3800, Australia
[c] Electron Microscopy Center, Chongqing University, Chongqing 400044, PR China
[d] CSIRO Manufacturing, Clayton, Victoria 3168, Australia

ARTICLE INFO

Article history:
Received 7 April 2018
Received in revised form 29 May 2018
Accepted 7 June 2018
Available online xxxx

Keywords:
Magnesium alloys
Stacking fault
Segregation
HAADF-STEM
DFT

ABSTRACT

Stacking faults in magnesium alloys have received considerable attention in recent years, but only intrinsic and extrinsic faults are studied at experimental and computational levels. Twin-like fault, designated as T_2 fault, has received little attention. In this study, we report for the first time the occurrence of T_2 fault in Mg–9.8 wt% Sn alloy. The T_2 fault and solute segregation in regions surrounding the fault were characterized using aberration-corrected scanning transmission electron microscopy and first-principles calculations. Sn atoms orderly distribute in the fault plane and its neighbouring planes, which drastically decreases the T_2 fault energy.

Stacking faults in magnesium and its alloys have attracted considerable attention in recent years [1–13]. They include intrinsic faults I_1 and I_2 and extrinsic fault E [14]. The I_1 fault has two Frank partial dislocations of $1/6\langle 02\bar{2}3\rangle_\alpha$ bounding its two ends. Its formation involves two different mechanisms. One is to remove a closely-packed plane A (or B) by vacancy condensation, and shear the planes above the removed plane by $1/3\langle 01\bar{1}0\rangle_\alpha$. The other is to dissociate a $\langle \boldsymbol{c}+\boldsymbol{a}\rangle$ perfect dislocation [9, 10, 13]. The I_2 fault is bounded by two Shockley partial dislocations. It is produced by shearing a part of the hcp lattice by $1/3\langle 01\bar{1}0\rangle_\alpha$, or dissociating an $\langle \boldsymbol{a}\rangle$ perfect dislocation [8, 10, 14]. The E fault is bounded by Frank partial dislocations of $1/2\langle 0001\rangle_\alpha$. It can form by inserting an extra C plane into the hcp stacking sequence, or by the dissociation of a $\langle \boldsymbol{c}\rangle$ perfect dislocation [14, 15]. Apart from these three types of stacking faults, the fourth type, twin-like (T_2) fault, has received only some theoretical attention [1, 2, 5–7, 16–18]. The T_2 fault changes the stacking sequence from ABABABAB to ABABCBABA, or BABACABAB, and hence it leads to a twin-like arrangement of closely-packed planes with respect to the fault plane C. This fault has been thought to form from an I_2 [1, 5, 7]. However, all previous studies of T_2 fault were made based on first-principles density functional theory (DFT) calculations, and no experimental evidence has thus far been reported for their existence. These studies reported that the T_2 has higher energy than I_1 and I_2 but lower energy than the E in pure magnesium [1, 2, 5, 7]. Since the E has already been detected experimentally in pure magnesium [12] and a Mg–Zn–Y alloy [10], the T_2 might also exist in some magnesium alloys. In this paper we report, for the first time, the existence of T_2 in a Mg–9.8 wt% Sn alloy that was artificially aged, or electron-beam irradiated in a transmission electron microscope. The T_2 is always associated with ordered Sn segregation.

Alloy with a nominal composition of Mg–9.8Sn (wt%) was cast using the method reported in our previous study [19]. Specimens cut from the ingot were heat treated at 300 °C for 24 h, 400 °C for 24 h, then solution treated at 500 °C for 4 h, followed by quenching to water at room temperature. Artificial ageing treatments were conducted in silicone oil at 100 °C for 720 h. Thin foil specimens for high-angle annular dark-field scanning transmission electron microscopy (HAADF-STEM) were prepared by mechanical polishing and ion-beam milling. HAADF-STEM images were acquired in a Cs-corrected FEI Titan G^2 60–300 ChemiSTEM operated at 300 kV. A thin area of about 20 μm^2 of a solution treated and water quenched specimen was irradiated with a spread electron-beam for 1 h in the TEM mode.

To calculate the generalized stacking fault energies (GSFEs) of T_2 in pure magnesium and Mg–Sn alloys, first-principles calculations based on DFT were performed within the Vienna Ab Initio Simulation Package (VASP) code [20] using the Generalized-Gradient Approximation exchange correlation functional of Perdew-Burke-Ernzerhof [21]. Atoms were treated using projector augmented-wave (PAW) pseudopotentials provided with VASP [22, 23]. The *k*-point meshes were constructed using the Monkhorst-Pack scheme [24]. To avoid interactions between two faults, a supercell containing 160 atoms and

* Corresponding author at: College of Materials Science and Engineering, Chongqing University, Chongqing 400044, PR China.
** Correspondence to: J.-F. Nie, Department of Materials Science and Engineering, Monash University, Victoria 3800, Australia.
E-mail addresses: hwchen@cqu.edu.cn, (H. Chen), jianfeng.nie@monash.edu (J.-F. Nie).

https://doi.org/10.1016/j.scriptamat.2018.06.018
1359-6462/

20 $(0002)_\alpha$ planes was used, with the three principal vectors of the supercell being parallel to $[2\bar{1}\bar{1}0]_\alpha$, $[01\bar{1}0]_\alpha$ and $[0001]_\alpha$. Ionic relaxations were allowed to occur along $[0001]_\alpha$. The T_2 was generated by displacing the eighth $(0002)_\alpha$ plane by $1/3[0\bar{1}10]_\alpha$. For one Mg–Sn alloy, one Mg atom on the eighth $(0002)_\alpha$ plane was replaced by Sn giving a supercell of $Mg_{159}Sn_1$. Since the T_2 is always associated with an ordered segregation of Sn similar to those in the β′-Mg_3Sn metastable phase [25], the GSFE to generate a T_2 in another Mg–Sn alloy with ordered Sn segregation was also calculated. This second supercell was constructed so that the configuration of Sn was similar to that in β′-Mg_3Sn, giving an atomic composition of $Mg_{150}Sn_{10}$. All values of the fault energies (E_F) were calculated according to the following equation:

$$E_F = E_T - N_{Mg}E_{Mg} - N_{Sn}E_{Sn(sol)}$$

where E_T is the total energy of a supercell, N_{Mg} and N_{Sn} are the numbers of Mg and Sn atoms in the supercell, respectively, E_{Mg} is the energy per Mg atom in pure magnesium, and $E_{Sn(sol)}$ is the energy per Sn atom in magnesium solution.

Fig. 1 shows atomic-resolution HAADF-STEM images of two T_2 faults in aged samples. These two faults were both on the C planes. Closer examination reveals that some atomic columns in each of these two fault planes deviate slightly from their original positions of the α-Mg lattice. Yellow arrows in the image indicate four of the deviated columns at the ends of the faults. The displacement of these atomic columns is along the $[1\bar{1}00]_\alpha$ direction, which is exactly the displacement required to move these atomic columns from position A to position C. The fault shown in Fig. 1a is only partially formed—only some columns have transformed from position A to position C and there are still two columns at position A in the fault plane, as marked by purple arrows. Around the partially formed fault, there was an ordered Sn segregation—the Sn-rich columns and Mg columns distribute alternately in the fault plane and its neighbouring planes, except those two untransformed columns, and those Sn-rich columns are symmetrical to the fault plane. The fault shown in Fig. 1b is fully formed. At the left side of this fault, there is a GP zone. The formation of GP zones in this alloy has been reported in our previous study [25]. Sn segregation around each fault is also visible and the arrangement of Sn-rich columns is again ordered and symmetrical. While the ordered and symmetrical features around the T_2 fault are similar to those in twin-related variants of β′-Mg_3Sn precipitates [25], the T_2 fault is structurally distinctive from the β′ precipitate. For the stacking sequence of closely-packed planes of ABABABA of Mg lattice, the T_2 fault has to be in plane C when it forms inside the Mg lattice. Although the formation of the T_2 also results in a symmetrical arrangement of closely-packed planes with respect to the T_2 fault plane (C plane, which is a twin plane), the stacking sequence of the closely-packed planes at each side of the T_2 fault plane is ABABAB only, i.e. there is no ABCA stacking sequence that is structurally identical to that of the β′ phase. The formation of the twin-related β′ variants changes the stacking sequence from BABABAB to BAC*B*CAB, where the italic letter *B* represents the twin plane. Note that the twin plane in this case is always B or A, and that there is a β′ unit at each side of the twin plane.

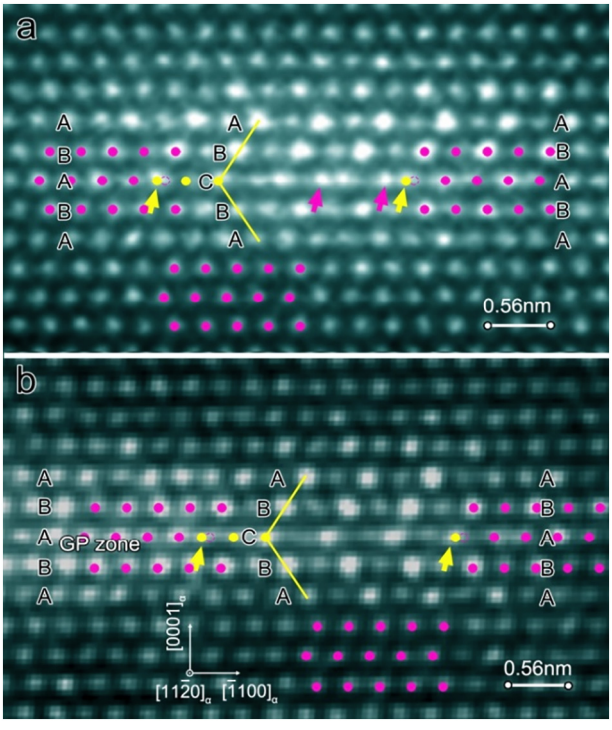

Fig. 1. Atomic-resolution HAADF-STEM images showing (a) a partially formed T_2 fault and (b) a fully formed T_2 fault in samples aged at 100 °C for 720 h. Purple solid dots indicate positions of periodic columns of α-Mg lattice and purple hollow dots indicate positions of some columns that used to be at position A in α-Mg lattice. Yellow solid dots indicate positions of some columns at position C in fault planes. Two purple arrows mark two untransformed atomic columns in (a). Yellow arrows mark some columns in the fault planes that slightly deviate from the periodic positions of the α-Mg lattice. A, B and C represent stacking sequence of the closely packed planes. Electron beam is parallel to $[11\bar{2}0]_\alpha$. (For interpretation of the references to color in this figure legend, the reader is referred to the web version of this article.)

T_2 were not frequently detected in aged samples. But many T_2 were found when thin foils of solution treated and water quenched samples were irradiated by electron beam for 1 h. Fig. 2a shows a HAADF-STEM image of such T_2 faults, as marked by yellow arrows. It is common to observe the existence of paired T_2 faults, with a separation distance of $3d_{(0002)_\alpha}$ between the two faults in the pair, Fig. 2b, as circled by yellow solid line ellipses in Fig. 2a. Occasionally, T_2 pairs with spacing of $5d_{(0002)_\alpha}$, Fig. 2c, were also found, as circled by yellow dashed line ellipses in Fig. 2a. Fig. 2b shows an enlarged HAADF-STEM image of a T_2 pair with spacing of $3d_{(0002)_\alpha}$. The closely-packed planes have a stacking sequence of BACABCBA, with the two T_2 faults lying on the C plane. The atomic columns in each of these two fault planes have slightly deviated from their original positions in the α-Mg lattice, as marked by yellow arrows in Fig. 2b. The deviation directions in these two fault planes are opposite—it is in the $[\bar{1}100]_\alpha$ direction in the top fault but $[1\bar{1}00]_\alpha$ in the bottom fault. Again, an enrichment of Sn atoms is visible around these two T_2 faults. While the Sn-rich columns in the region between the two T_2 faults have a distribution resembling that in β′-Mg_3Sn and the local stacking sequence of closely-packed planes (CABC) is similar to that of a four-layer structure of β′, the T_2 pair is intrinsically different from β′, because the stacking sequence of β′ has to be BCAB or ABCA (Figs. 2d and 3d), rather than CABC, when it forms inside the Mg lattice with the ABABAB stacking sequence. Furthermore, there is a Shockley partial at the end of β′, but no Shockley at the end of the T_2 pair.

Based on images shown in Figs. 1 and 2, the formation mechanism of the T_2 is proposed to involve displacement of atomic columns from their positions in a closely-packed plane of A or B to positions in C. For α-Mg lattice, the magnitude of this displacement is $1/3\langle 10\bar{1}0\rangle_\alpha$. Since there are three crystallographically equivalent directions of $\langle 10\bar{1}0\rangle_\alpha$, i.e., $[10\bar{1}0]_\alpha$, $[0\bar{1}10]_\alpha$ and $[\bar{1}100]_\alpha$, there are three different paths to generate a T_2. When the electron beam is parallel to $[11\bar{2}0]_\alpha$, the whole magnitude of $1/3[\bar{1}100]_\alpha$ displacement is projected onto the $(11\bar{2}0)_\alpha$, since the displacement direction is perpendicular to the electron beam. For $1/3[0\bar{1}10]_\alpha$ or $1/3[10\bar{1}0]_\alpha$ displacement that is at 30° to the electron beam, only half of its magnitude is projected onto $(11\bar{2}0)_\alpha$. Thus, those displacements that generate the T_2 in Figs. 1 and 2 are actually $1/3[0\bar{1}10]_\alpha$ or $1/3[10\bar{1}0]_\alpha$ due to their magnitudes being $1/6[1\bar{1}00]_\alpha$ on $(11\bar{2}0)_\alpha$. Fig. 3a show formation mechanism of a T_2. This fault is generated by displacing some atomic columns by $1/3[0\bar{1}10]_\alpha$ in